Journal of Materials Science: Materials in Electronics (2019) 30:17363–17373
https://doi.org/10.1007/s10854-019-02085-3

Transport and magneto-transport properties in $La_{0.8}K_{0.2-x}\square_xMnO_{3-\delta}$ ($x=0$ and 0.1) manganites

R. Skini[1] · P. Svedlindh[1] · E. Dhahri[2] · E. K. Hlil[3]

Received: 9 May 2019 / Accepted: 21 August 2019 / Published online: 4 September 2019

Abstract
We discuss the effect of the nanometric grain size on the behavior of the electrical and magnetoresistive response of $La_{0.8}K_{0.2-x}\square_xMnO_{3-\delta}$ ($x=0$ and 0.1) nanocrystalline samples that were prepared by a sol–gel method. The results from transport and magneto-transport measurements evidence a robust dependence on the nanometric grain size. The temperature dependence of the resistivity was evaluated using different transport models. The results reveal a field-dependent minimum of the resistivity in the low-temperature region, which can be described in terms of intergranular spin-polarized tunneling. Remarkably, a considerable increase of the magnetoresistance (MR) with the decrease of nanoparticle size was found, which might open a new way for the search for potential candidates for magnetoresistive devices. Besides, the magnetic field dependence of the MR was also analyzed, and a distinct drop of MR at low fields was noticed. This behavior was primarily explained by the spin-polarized tunneling transport of conduction electrons across grain boundaries.

1 Introduction

Magnetic materials with remarkable magnetotransport features have awakened much interest over the past years by introducing fundamental challenges as well as opening novel venues for new magnetic applications [1, 2]. Examples of these materials are the well-known manganites with the general formula $R_{1-x}A_xMnO_3$ (R = rare-earth, and A = divalent element). Indeed, the perovskite structure of these materials has attracted so much interest given their uncommon transport and magnetotransport properties [3–5], charge ordering, orbital ordering, and phase separation [6].

The origin of ferromagnetism for materials like $La_{0.8}A_{0.2}MnO_3$ (A = Ca, Sr, Na, K…) exhibiting the colossal magnetoresistance (CMR) effect, is typically ascribed to the double-exchange mechanism [7]. The sole nature of double-exchange mediated ferromagnetism leads to very high spin polarization of the conduction electrons in the ferromagnetic (FM) state, thus making these materials promising candidates for magnetoresistive devices. Nevertheless, in the case of epitaxial thin films and ceramic CMR materials, magnetic fields of several Tesla are generally needed to obtain the CMR response close to the FM Curie temperature (T_C) [8, 9], and hence restricting the potential of these materials for applications. A question then arises as to the technological relevance of the manganites. One apparent setback is the high resistivity close to T_C, resulting in considerable voltage noise in any real field-sensing device. What is trustworthy to mention is that the CMR in manganites is principally linked to the intrinsic properties of the system while the extrinsic ones correspond to the so-called low-field MR (LFMR). This CMR is mainly attributed to the existence of interfaces and grain boundaries [8–11]. A key feature deduced at temperatures much below T_C is the negative MR at low fields followed by a more modest increase of the MR with the increase in the magnetic field at high fields [high-field MR (HFMR)]. The LFMR noted at low temperature was explained by the spin-polarized tunneling transport of conduction electrons across grain boundaries [3, 8, 12]. Although the LFMR seems to be promising for possible sensor applications, recent research works have shown that the effect is prominent only at low temperatures, sharply dropping with the increase in temperature [8–11, 13]. Near room temperature, this effect nearly disappears because the high degree of spin polarization, caused by the

✉ R. Skini
ridha.skini@angstrom.uu.se

[1] Department of Engineering Sciences, Uppsala University, Box 534, 751 21 Uppsala, Sweden

[2] Laboratoire de Physique Appliquée, Faculté des Sciences de Sfax, Université de Sfax, B.P. 802, Sfax 3018, Tunisie

[3] Institut Néel, CNRS et Université Joseph Fourier, BP 166, 38042 Grenoble Cedex 9, France

half-metallic nature of these materials, remains only in the low-temperature FM regime.

To further understand this behavior, the impact of nanometric grain size on the transport and magnetoresistance response of $La_{0.8}K_{0.2-x}\square_xMnO_{3-\delta}$ ($x=0$ and 0.1) nano-sized manganites was explored.

2 Experimental details

Nanocrystalline samples $La_{0.8}K_{0.2-x}\square_xMnO_{3-\delta}$ ($x=0$ and 0.1) were prepared by the well-known sol–gel route. Stoichiometric amounts of the nitrate precursor reagents KNO_3, $La(NO_3)_3$ $6H_2O$ and $Mn(NO_3)_2$ $4H_2O$ were dissolved in water and mixed with citric acid and ethylene glycol, creating a steady solution. The molar ratio metal:citric acid was 1:1. The solution was treated at 80 °C under continuous stirring to eliminate excess water and get a viscous gel. The obtained gel was decomposed at 300 °C, and the resulting precursor powder was heated in air at 500 °C, 600 °C and 700 °C for 24 h to improve crystallinity. Afterward, the powder was pelletized and annealed at 700 °C for 12 h. The samples were quenched in air by removing the furnace.

The crystallinity and phase composition of the powders were checked by X-ray diffraction (XRD) using CuKα radiation ($\lambda = 1.5418$ Å). The magnetic measurements were carried out using the BS1 and BS2 magnetometers developed at Institut Néel in Grenoble. Transport and magnetotransport measurements were performed by a standard four-probe technique in a Quantum Design Physical Property Measurement System.

3 Results and discussions

The room temperature XRD results indicate a single-phase nature of both $La_{0.8}K_{0.2-x}\square_xMnO_{3-\delta}$ samples (Fig. 1a). The obtained results reveal that both samples have crystallized in the rhombohedral structure belonging to the $R\bar{3}C$ space

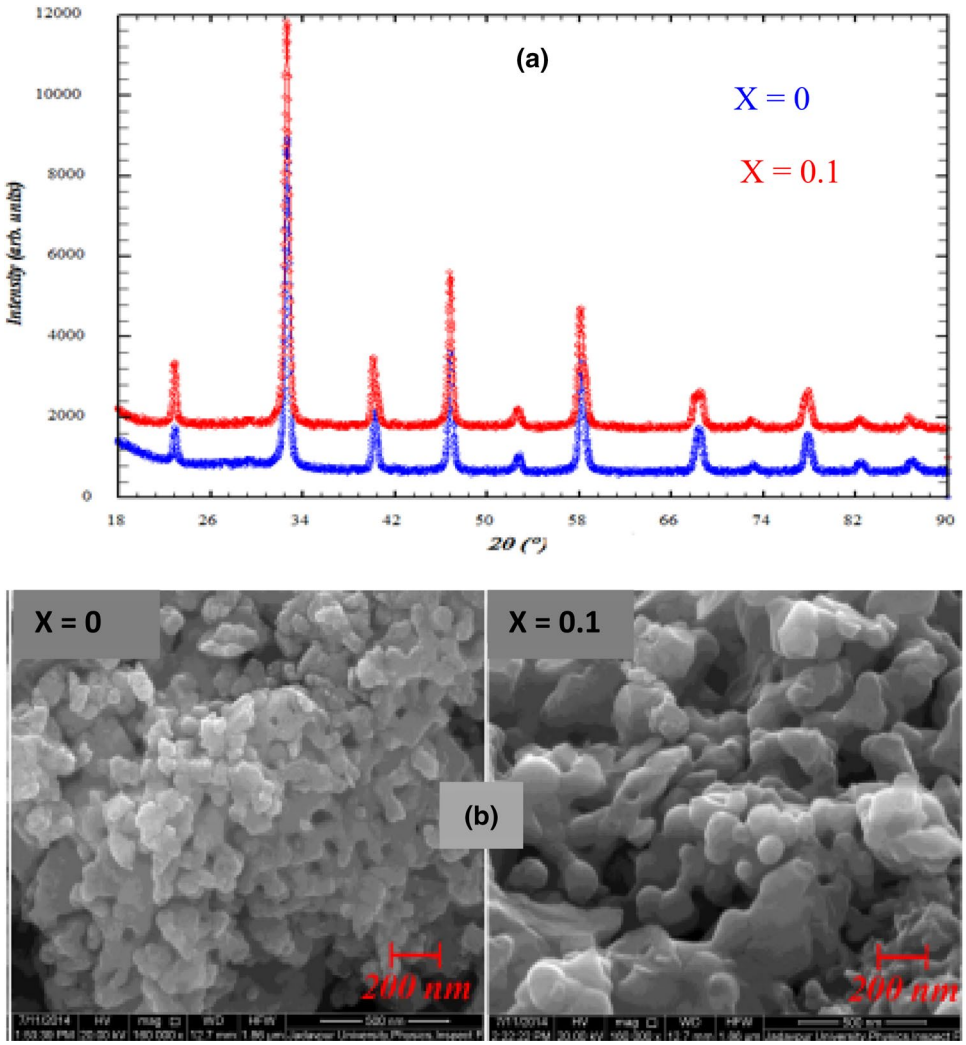

Fig. 1 **a** XRD patterns of $La_{0.8}K_{0.2-x}\square_xMnO_{3-\delta}$ ($x=0$ and 0.1) compounds at room temperature. **b** Evolution of the particle size with x in the nanocrystalline $La_{0.8}K_{0.2-x}\square_xMnO_{3-\delta}$ phase

group. The structural and magnetic properties have been reported earlier by us [14].

The average particle size was estimated by using the Debye–Scherrer formula:

$$D = 0.89\lambda/\beta\cos\theta, \quad (1)$$

where λ is the X-ray wavelength and θ is the diffraction angle. β is the full width at half maximum after subtracting the instrumental line broadening for the most intense diffraction peak,

$$\beta = \beta_m^2 - \beta_i^2, \quad (2)$$

where β_m^2 is the experimental full width at half maximum (FWHM) and β_i^2 is the FWHM of a standard silicon sample. The D values were found to be 50 and 69 nm for $x=0$ and 0.1 nanoparticle samples, respectively.

We used representative SEM images for the two samples (Fig. 1b) to again calculate the particle size, and the values were found to be 48 and 65 nm for $x=0$ and 0.1, which agree well with those estimated from the XRD analysis. Moreover, the geometric density (mass/volume) of the samples was determined to investigate how the sample resistivity depends on the sintered density. The relative sintered densities values were found to be 3.37 and 4.89 g/cm^3 for the $x=0$ and 0.1 nanoparticle samples, respectively. We have also calculated the porosity of the samples using the following equation [15]:

$$P(\%) = 100 \cdot \left(1 - d_{cal}/d_{th}\right),$$

where d_{cal} is the theoretical density and d_{th} is the calculated density. The obtained values were found to be 23 and 17%, for the $x=0$ and 0.1 nanoparticle samples, respectively.

From magnetic measurements, a second-order magnetic phase transition from the paramagnetic to the ferromagnetic state was observed. The Curie Temperature T_C decreased with increasing x, from 325 for $x=0$ to 300 K for $x=0.1$ [14].

Figure 2 shows the temperature (T) dependence of the zero field resistivity (T). It is to be noticed that the electrical resistivity presents a complex temperature variation; a low temperature minimum at around 50 K (T_{min}) followed by a maximum attributed to the metal–insulator transition at $T_{MI} = 270$ K and 235 K for $x=0$ and 0.1, respectively. Besides, a drop of the resistivity with the increase of grain size over the whole temperature range was observed, which affirms a strong dependence of the resistivity on grain size and the existence of grain boundaries that act as regions of disorder and enhanced scattering for the conduction electrons. Isaac et al. [16] and Sanchez et al. [17] have shown that the spins become disordered at the grain boundaries due to the strain, an effect that becomes more pronounced decreasing the grain size yielding an increase of the resistivity. Similarly, Das et al. [18] suggest that since the spins

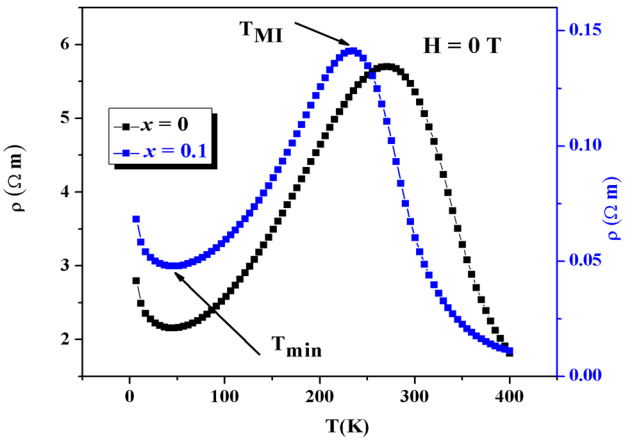

Fig. 2 Temperature (T) dependence of the zero field resistivity (T) for $La_{0.8}K_{0.2-x}\square_xMnO_{3-\delta}$ ($x=0$ and 0.1) with different grain sizes

are more disordered at grain boundaries than inside grains, the resistivity decreases with grain growth. As for Gupta et al. [19], the spin disorder was described as canting of Mn spins near the surface of the grains. Furthermore, a low temperature minimum of the resistivity in manganites has been the interest of several works [3–5]. Moreover, the obtained results have revealed a strong dependence on the number of potassium vacancies, particle size and the applied magnetic field. The Curie temperature as well as the temperature of the metal–insulator transition decrease with the introduction of potassium vacancies, which can be explained by either of the following two effects; increase of the Mn^{3+}/Mn^{4+} ratio or increase in the number of oxygen vacancies (δ). Moreover, the resistivity decreases significantly with the introduction of potassium vacancies. However, there are other effects contributing to the strong decrease of the resistivity for the $x=0.1$ sample; the increase of both the grain size and the sintered density (decrease of porosity). To understand the decrease of the resistivity for the x = 0.1 sample, one can adopt a simplified resistance network model including low resistance grains and high resistance grain boundaries [20]. Assuming that the resistivity of the sample is dominated by the grain boundary resistance, the much reduced resistivity for the x = 0.1 sample can be explained by the reduced resistance of grain boundaries due to larger grains and increased sintered density (decreased porosity); larger grains and increased sintered density will change both the dimensions and physical properties of grain boundaries to favor a decrease of the grain boundary resistance. It should be noted that the grain boundaries contribute with a temperature independent contribution to the sample resistivity.

To prove this dependence, we have investigated in detail the impact of external magnetic field on the temperature dependence of electrical resistivity for both samples in the low temperature (5 K < T < 70 K), ferromagnetic metallic

region (70 K < T < T_{MI}) and paramagnetic insulating region (T_{MI} < T < 400 K).

3.1 Low-temperature region (5 K < T < 70 K)

The resistivity behavior in the low-temperature region has generally been attributed to the competition of two contributions [21]. The first one is the Coulomb blockade effect (CB, electrostatic blockade of carriers between grains) [3, 5, 22, 23] of weak localization and strong electron–electron interactions within a disordered metallic state [4]. As for the second contribution, it pertains to the bulk scattering model, which includes a quantum correction to the conductivity. This model disagrees with the experimental data for ceramic manganites, whose low temperature resistivity minima are present even in a small magnetic field [21]. However, the intergranular spin-polarized tunneling model (ISPT) has been proposed for the strongly field dependent low-temperature resistivity minima [24]. According to this model, the resistivity minimum occurring at low temperature depends strongly on the grain size, and shifts towards lower temperature upon applying a magnetic field and disappears at some high magnetic field. The high field value depends strongly on the grain size and for some materials, the suppression of the minimum requires high magnetic field up to 14 T [21, 25, 26]. Considering the tunneling through the grain boundary, the functional form of resistivity is given by [25]:

$$\rho(T,H) = (\rho_0 + \rho_1 T^{3/2})/(1 + \varepsilon\langle\cos\theta_{ij}\rangle), \tag{3}$$

where ρ_0 and ρ_1 are field independent parameters and ε is linked to the degree of spin polarization of the charge carriers. For $H = 0$, the spin correlation function $\cos\theta_{ij}$ is expressed as follows:

$$\langle\cos\theta_{ij}\rangle = -L\big(|J_S|/k_BT\big) \tag{4}$$

Here, $L(x) = \left[\coth x - 1/x\right]$ is the Langevin function, J_S is the intergrain antiferromagnetic exchange integral and k_B is the Boltzmann constant. For $H \neq 0$, the analytical expression for spin correlation function of the classical Heisenberg model for ultra-small systems of spins, interacting via isotropic, nearest-neighbor (n–n) exchange can be expressed as [27]:

$$\langle\cos\theta_{ij}\rangle = \frac{1}{4} + \frac{1}{3 + \exp\left(\frac{-3J_s}{k_BT}\right)}, \tag{5}$$

where $g\mu_B H/J_S = \frac{3}{2}$.

As we mentioned above, the resistivity minimum has also been attributed to the CB effect. Indeed, Sheng et al. came to the conclusion that the expression describing the increasing nature of resistivity at low temperature is given by:

$$\rho(T) = A\exp\left(\sqrt{\Delta/k_BT}\right), \tag{6}$$

where A is a fitting parameter and $\Delta \sim E_c$ is the energy barrier [28]. Several works have focused on the existence of the CB contribution in the resistivity of manganites. Balcells et al. [23] have proven the presence of the CB contribution in the resistivity of granular $La_{0.7}Sr_{0.3}MnO_3$. Furthermore, Dey et al. proposed that the transport mechanism of $La_{0.7}Ca_{0.3}MnO_3$ nanocrystalline samples with particle sizes 14-27 nm is governed by the CB effect [4]. Physically, the CB effect cannot describe the strongly field-dependent minima of the resistivity at low temperature. In our case, we note that the minima of the resistivity are strongly affected by the magnetic field. Indeed, the resistivity minimum becomes more shallow with the increase of the external magnetic field. Hence, it can be concluded that the ISPT model is primarily responsible for the resistivity minimum at low temperature for the $La_{0.8}K_{0.2-x}\square_xMnO_{3-\delta}$ ($x = 0$ and 0.1) nanocrystalline manganites samples. The $\rho(T)$ curves are fitted to Eq. (3) using the expression for $\cos\theta_{ij}$ in Eqs. (4) and (5). Excellent fits are obtained for both samples (Fig. 3). The best fitted parameters ρ_0, ρ_1, ε and J_S are given in Table 1.

3.2 Ferromagnetic metallic region (70 K < T < T_{MI})

In the ferromagnetic metallic region, the magnetic moments of neighboring $Mn^{3+}\left(t_{2g}^3 e.g.^1 : S = 2\right)$ and $Mn^{4+}\left(t_{2g}^3 e.g.^0 : S = 3/2\right)$ ions are ferromagnetically coupled through the double-exchange mechanism [29, 30]. The temperature dependent resistivity data was proven to match well with an empirical equation of type $\rho = \rho_0 + \rho_n T^n$, where ρ_0 is the residual resistivity due to the domain boundaries and other temperature-independent scattering mechanisms [31].

In the metallic region, depending on the scattering mechanism the transport mechanism is commonly described by one of the following equations:

$$\rho(T) = \rho_0 + \rho_{2.5}T^{2.5}, \tag{7}$$

$$\rho(T) = \rho_0 + \rho_2 T^2 + \rho_{4.5}T^{4.5}, \tag{8}$$

$$\rho(T) = \rho_0 + \rho_2 T^2 + \rho_5 T^5, \tag{9}$$

where $\rho_{2.5}T^{2.5}$ is the electrical resistivity due to electron-magnon scattering in the ferromagnetic phase [32]. The term $\rho_2 T^2 + \rho_{4.5}T^{4.5}$ is a combination of electron–electron, electron-magnon and electron–phonon scattering processes [33, 34], while the $\rho_2 T^2 + \rho_5 T^5$ term is ascribed to the electron–electron and electron–phonon interactions [35]. To find the appropriate equation elucidating the transport mechanism, we fitted the experimental results of the samples under investigation using these equations. We can deduce that the best fit is obtained using Eq. (9), indicating that the transport

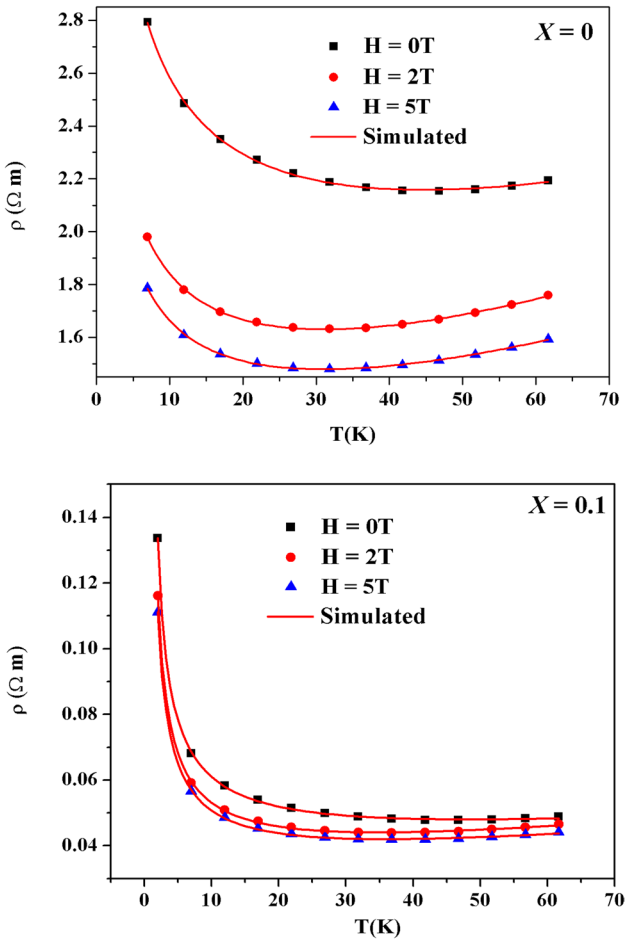

Fig. 3 Variation of resistivity (ρ) with temperature for $La_{0.8}K_{0.2-x}\square_xMnO_{3-\delta}$ ($x=0$ and 0.1) in the temperature range of 0–70 K under different applied magnetic fields. Symbols are the experimental results and solid lines are fits of the experimental data using Eq. (3)

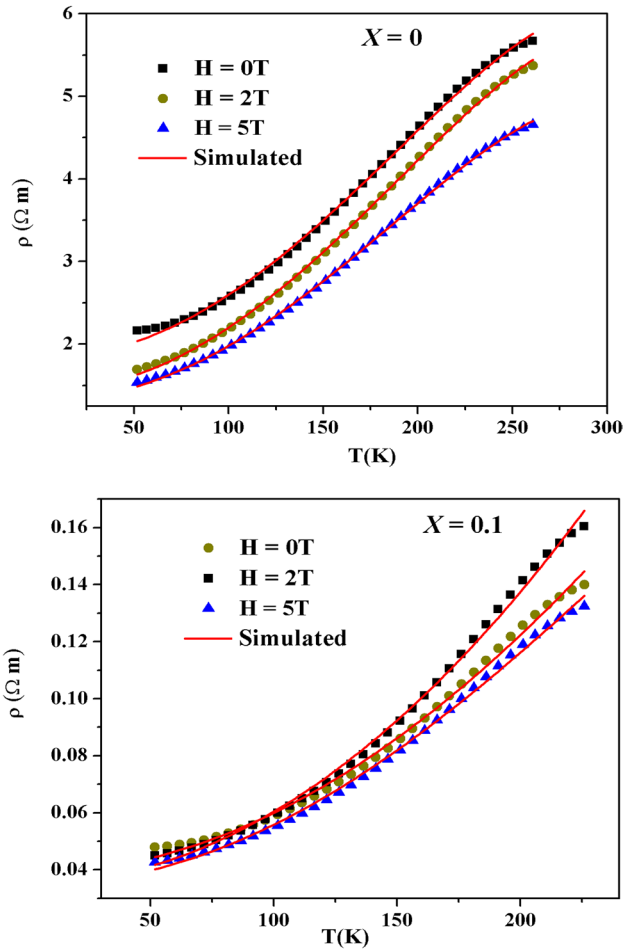

Fig. 4 Resistivity versus temperature for $La_{0.8}K_{0.2-x}\square_xMnO_{3-\delta}$ ($x=0$ and 0.1) in the metallic region under different applied magnetic fields. Symbols are the experimental results and solid lines are fits of the experimental data using Eq. (9)

Table 1 Best-fit parameters obtained from intergranular tunneling model

H (Tesla)	ρ_0 (10^{-2} Ωm)	ρ_1 (10^{-2} Ωm $K^{-3/2}$)	ε	*Js* (meV)
x = 0				
0	1.908	3.276×10^{-4}	0.465	1.823
2	1.361	6.232×10^{-4}	0.457	1.786
5	1.242	5.523×10^{-4}	0.449	1.758
x = 0.1				
0	0.445	2.641×10^{-6}	0.834	0.855
2	0.0387	1.064×10^{-5}	0.839	0.836
5	0.0371	9.098×10^{-6}	0.840	0.827

mechanism in the intermediate temperature region is governed by the electron–electron and electron–phonon scattering processes (Fig. 4).

3.3 Paramagnetic insulating region ($T_{MI} < T < 400$ K)

It has been recognized that the electronic transport in the high-temperature region is controlled by the small polaron hopping mechanism, in which the resistivity follows the relation below [36]

$$\rho(T) = A\exp(E_a/k_BT), \tag{10}$$

where A is a pre-exponential coefficient and E_a is the activation energy.

Figure 5 demonstrates the validity of the small polaron hopping mechanism through a linear dependence of Ln (ρ/T) as a function of T^{-1}. The activation energy E_a was found to be 0.174 and 0.204 eV for $x=0$ and 0.1 samples, respectively.

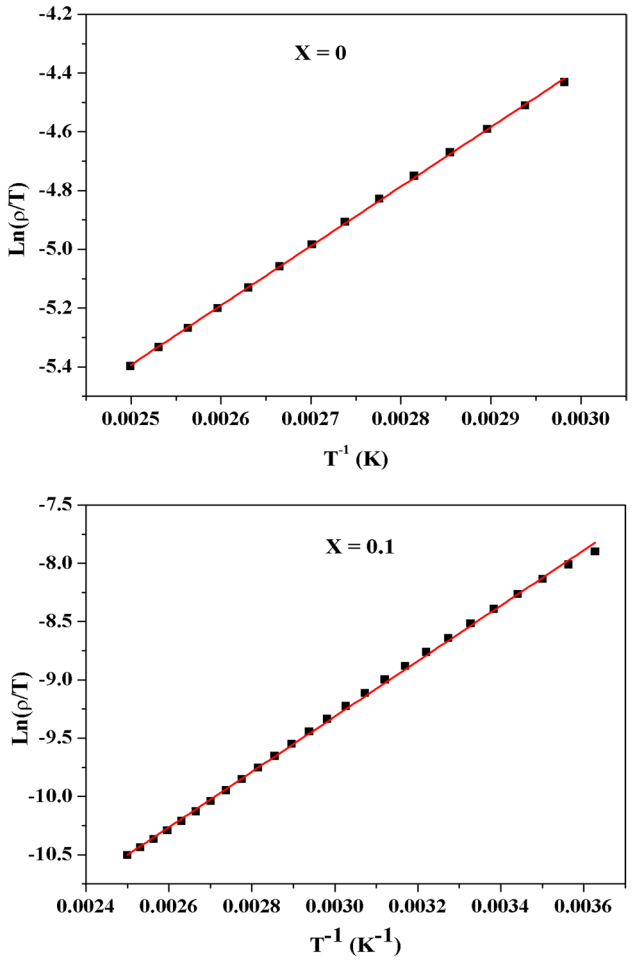

Fig. 5 Temperature dependence of resistivity for $La_{0.8}K_{0.2-x}\square_xMnO_{3-\delta}$ ($x=0$ and 0.1) in the paramagnetic insulating region. The line represents the fit according to Eq. (10)

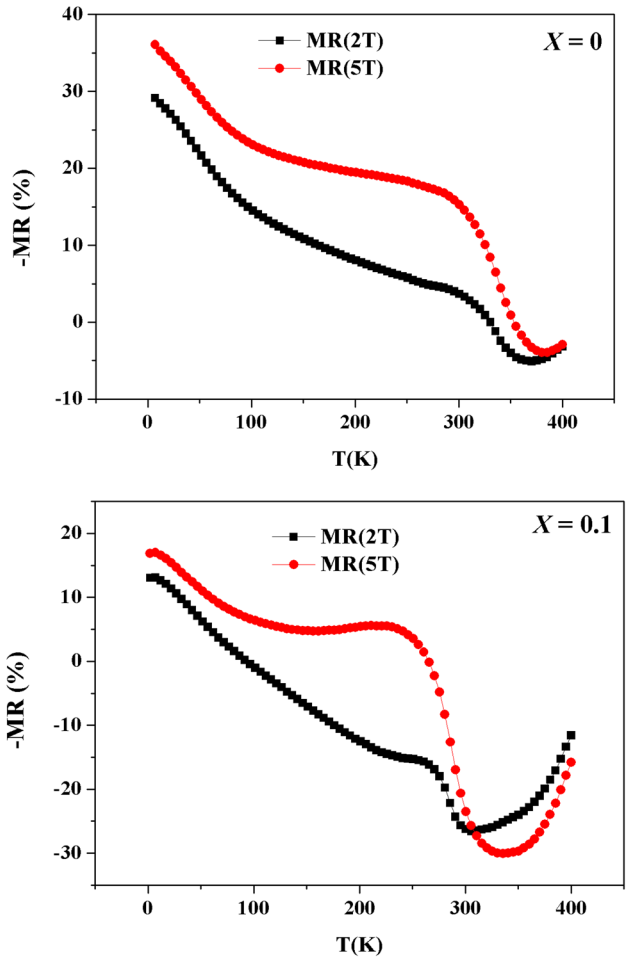

Fig. 6 Magnetoresistance (*MR*) versus temperature for $La_{0.8}K_{0.2-x}\square_xMnO_{3-\delta}$ ($x=0$ and 0.1) samples under different external magnetic fields

3.4 Magnetoresistance properties

The magnetoresistance (MR) defined as the change of electrical resistance in the presence of a magnetic field is characterized by two contributions that are different [37]. The first one is the intrinsic MR (MR_{INT}), which is explained by the double exchange mechanism, noted near the ferromagnetic–paramagnetic transition temperature T_C and resulting from the suppression of spin fluctuations by aligning the spins on the application of the magnetic field. The resistivity at low temperature gives rise to another type of MR defined as an extrinsic MR contribution (MR_{EXT}), which can be explained by the intergranular spin-polarized tunneling model (ISPT) across the grain boundaries (GBs).

Figure 6 shows the temperature dependence of the magnetoresistance $MR = (R(H) - R(0))/R(0)$ of the $La_{0.8}K_{0.2-x}\square_xMnO_{3-\delta}$ ($x=0$ and 0.1) nanocrystalline samples under different applied magnetic fields. The results reveal an unusual magnetoresistance for both samples characterized by a negative *MR* at low temperature followed by a decline of the *MR* with the increase of temperature and the *MR* turning positive at higher temperatures. Consequently, the samples exhibit competition between MR_{INT} and MR_{EXT} by revealing a small peak in the MR observed around T_{MI} and a *MR* switching sign on cooling. The low temperature magnetoresistance is explained by taking into account the ISPT through the GBs [3, 5, 38]. Applying a magnetic field results in magnetic domain wall motion through grain boundaries, progressive alignment of magnetic domains and consequently a decrease of the resistance (negative *MR*). A substantial rise of the low temperature magnetoresistance was detected with the decrease of nanoparticle size, paving the way to discover potential candidates for magnetoresistive devices.

The *MR* has also been investigated as a function of the magnetic field (Fig. 7). The curves reveal two different variations. A distinct drop of MR was noticed at low fields ($H < 1$ T), followed by a weaker change of the

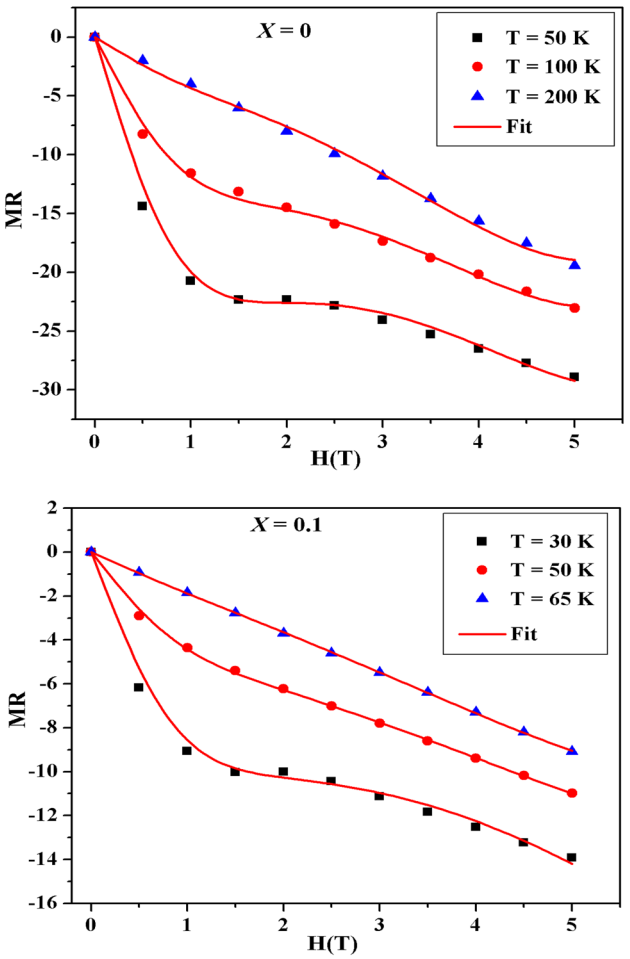

Fig. 7 Magnetoresistance (*MR*) versus magnetic field for $La_{0.8}K_{0.2-x}\square_xMnO_{3-\delta}$ ($x=0$ and 0.1). Symbols are the experimental results and solid lines are fits of the experimental data using Eq. (11)

MR at higher fields, where the MR is almost linear with *H*. Therefore, it is interesting to separate the part of the MR originating from ISPT (MR_{ISPT}), from that of the MR determined by the suppression of spin fluctuations (MR_{INT}). Helman and Abeles described the dependence of the MR on the magnetic field considering the gradual slippage of domain walls across the grain boundary pinning centers [24]. Once more, Raychaudhuri et al. proposed a relevant model based on ISPT transport of conduction electrons at the grain boundaries [10]. Following their model, the expression for the MR is as follows:

$$MR = -\tilde{A}\int_0^H f(k)dk - JH - KH^3 \tag{11}$$

where *J* and *K* are field independent constants, *k* is the depinning field at grain boundaries and *f*(*k*)describes the distribution of depinning fields. Following Raychaudhuri [9, 10], *f*(*k*) is taken as the weighted average of Gaussian and skewed Gaussian distributions,

$$f(k) = A\exp\left(-Bk^2\right) + Ck^2\exp\left(-Dk^2\right). \tag{12}$$

Using the values of the fitting parameters *A*, *B*, C, *D*, *J* and *K* ($\tilde{A}$ is absorbed in *A* and *C*), we can separate the MR_{ISPT} and MR_{INT} parts from the total MR as follows:

$$MR_{ISPT} = -\int_0^H f(k)dk, \tag{13}$$

$$MR_{INT} = -JH - KH^3. \tag{14}$$

The MR curves were fitted through a similar procedure to that considered by Raychaudhuri et al. [9, 10]. Hence, we differentiate Eq. (11) with respect to *H,* using Eq. (12),

$$d(MR)/dH = A\exp\left(-BH^2\right) + CH^2\exp\left(-DH^2\right) - J - 3KH^2. \tag{15}$$

Figure 8 shows the derivative of the experimental MR versus magnetic recorded at different temperatures and fitted using Eq. (15).

Using the extracted fitting parameters, we have calculated the *MR* as a function of *H* from Eq. (11), the results are presented in Fig. 7. Also, by using the fitting parameters, we have calculated the temperature dependence of MR_{ISPT} and MR_{INT} for both samples using Eqs. (13) and (14), respectively, the results are presented in Fig. 9 a, b, respectively. At $T=50$ K, a drop of MR_{ISPT} with the increase of the particle size was detected. Indeed, it has been reported that MR_{ISPT} is very sensitive to the grain boundary effects, and is expected to continue increasing with the decrease in particle size [3, 4]. Therefore, to explain the fundamental physics behind this unusual temperature dependence of MR, one needs to pay special attention to the surface magnetization of the grains (MR_{surf}).

To analyze the relevance of MR_{surf} in the present case of nanogranular manganites, it is prerequisite to consider the nanometric grain size of our samples for which the surface-to-volume ratio of each grain is adequately large. Previous works have proven that the magnetic behavior in the nanosized regime is commonly controlled by the surface magnetic properties, increasing in importance with with the increase in the surface-to-volume ratio [39–41]. Nonetheless, up to now, the central key of the grain surface region in manganites is still not well understood. For instance, Park et al. [42] have found that MR_{surf} is suppressed compared to the bulk magnetization, while, Soh et al. [43] have reported that the magnetic ordering temperature for the grain boundary spins increases by as much as 20 K compared to the bulk T_C value. To explain such a phenomenon, the theoretical model developed by Lee et al. [13] was used. According to their model, the magnetoconductivity (σ) as a function of the magnetic field is given by:

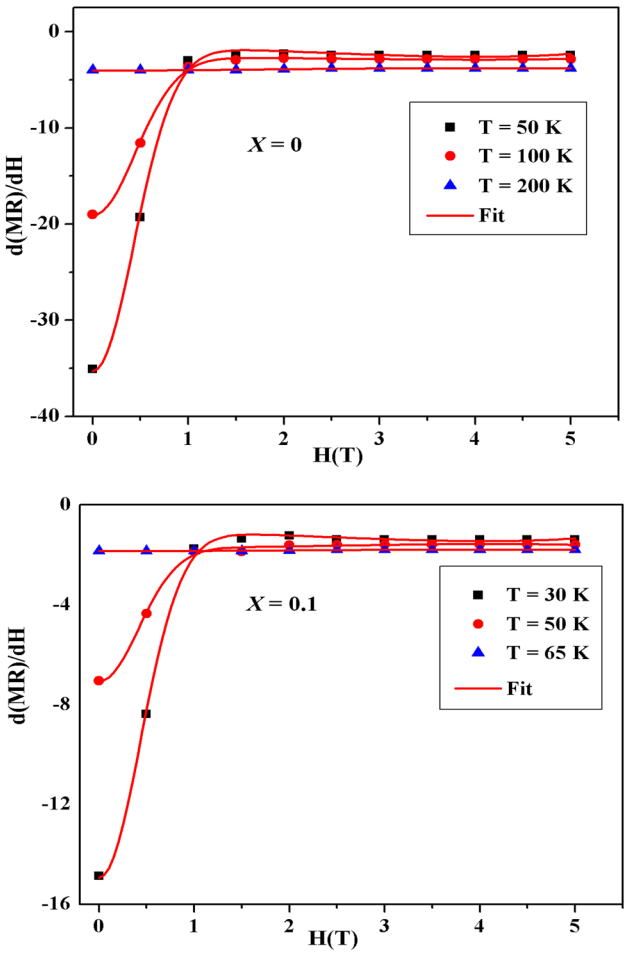

Fig. 8 Magnetic field derivative of the experimental *MR*(*H*) for $La_{0.8}K_{0.2-x}\square_xMnO_{3-\delta}$ ($x=0$ and 0.1). Symbols are the experimental results and solid lines are fits of the experimental data using Eq. (15)

$$\sigma/\sigma_0 \propto 1 + 2\overrightarrow{M}\cdot\langle\widehat{S_b}\rangle + \langle\left(\vec{M}\cdot\widehat{S_b}\right)^2\rangle, \tag{16}$$

where σ_0 is the zero-field conductivity, $\hat{S}_b$ is the spin orientation at the grain boundary, and $\vec{M}$ is a vector describing the direction of the bulk magnetization. At high fields, averaging over possible angles between the bulk and surface magnetizations Eq. (16) reduces to,

$$\sigma/\sigma_0 \approx 1 + \frac{1}{3}M^2 + 2\chi_b HM. \tag{17}$$

The thermal average of the boundary spin is proportional to $\chi_b\vec{H}$, where χ_b is the spin susceptibility of the boundary spins. Hence, the magnetoconductivity $MC = \sigma(H)/\sigma_0$ was calculated as a function of temperature and magnetic field for the $La_{0.8}K_{0.2-x}\square_xMnO_3$ ($x=0$ and 0.1) samples, the results are presented in Fig. 10a, b. As stated by this model, the slope (S) of the *MC* versus *H* curve in the high-field region (H > 2 T) can be taken as the measure of the surface spin susceptibility χ_b. Figure 10c, d show the temperature dependence of surface spin susceptibility (S) of both samples. It was discovered that S(T) is qualitatively similar to that of *MR(T)*, affirming that the MR_{surf} is a major key factor in determining the transport and magnetotransport properties of nanogranular $La_{0.8}K_{0.2-x}\square_xMnO_{3-\delta}$ ($x=0$ and 0.1) manganites.

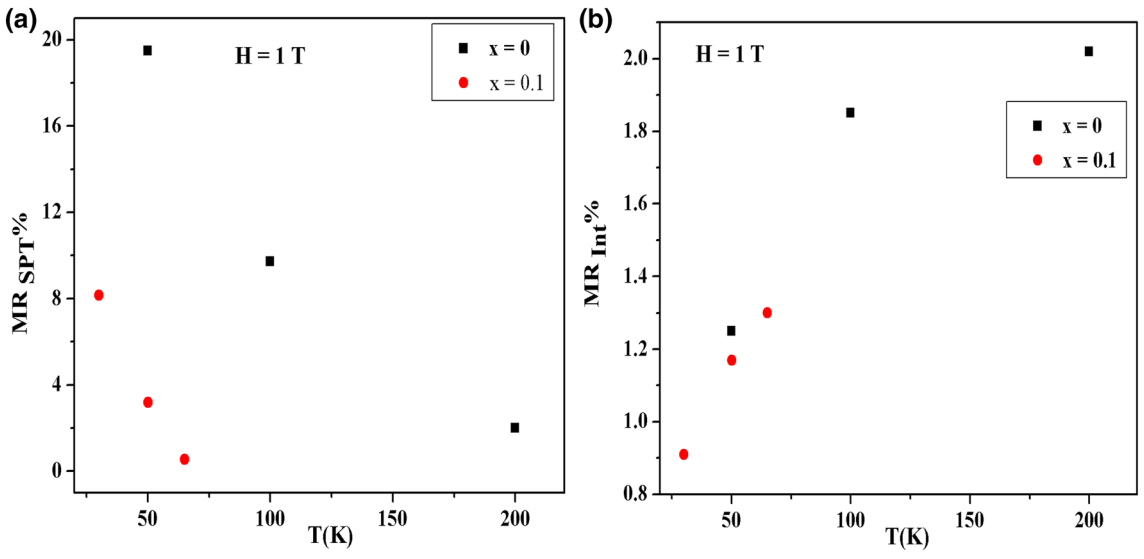

Fig. 9 **a** Temperature dependence of MR_{ISPT} for $La_{0.8}K_{0.2-x}\square_xMnO_{3-\delta}$ ($x=0$ and 0.1) at $H=1$T magnetic field. **b** Temperature variation of MR_{INT} for both compounds at the same magnetic field of $H=1$T

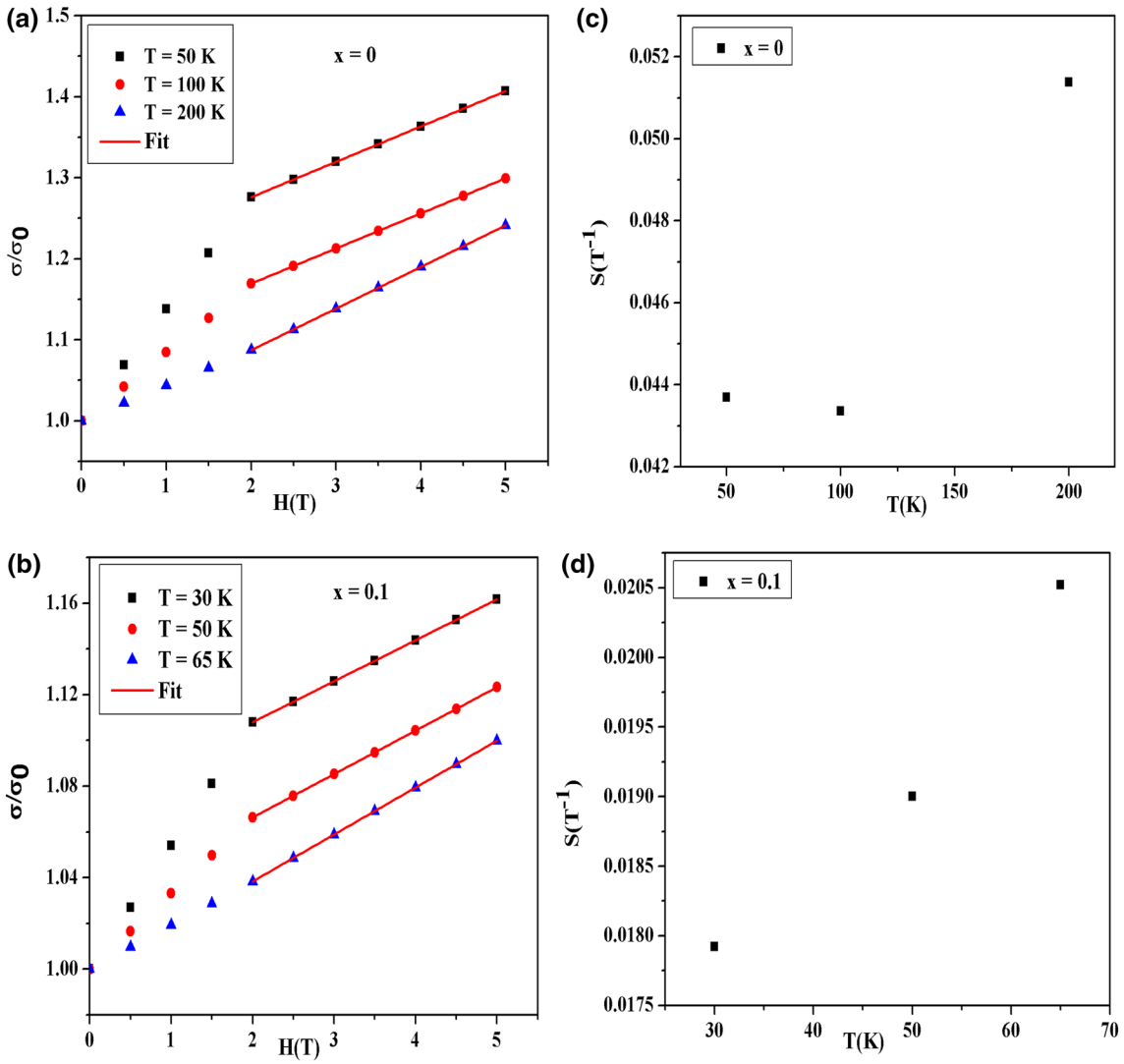

Fig. 10 **a** and **b** Magnetic field variation of magnetoconductivity $\sigma(H)/\sigma_0$ at several temperatures for $La_{0.8}K_{0.2-x}\square_xMnO_{3-\delta}$; **a** ($x=0$) and **b** 0.1. **c** and **d** Grain boundaries spin susceptibility S as a function of temperature for $La_{0.8}K_{0.2-x}\square_xMnO_{3-\delta}$ ($x=0$ and 0.1)

4 Conclusion

In the present research work, we have studied the how of the particle size affects transport and magnetotransport properties of nanogranular $La_{0.8}K_{0.2-x}\square_xMnO_{3-\delta}$ ($x=0$ and 0.1). Different models have been utilized to describe the transport properties of the samples in the whole temperature region. The low temperature MR has been explained by taking into account the intergranular spin-polarized tunneling occurring at the GBs. We have analyzed our experimental MR data following a phenomenological model to separate the MR arising from inter-grain spin-polarized tunneling (MR_{ISPT}) from the intrinsic contribution (MR_{INT}) in our samples. Finally, we examined the low and high field magnetoconductivity data of our samples. Interestingly, our experimental results indicate that MR_{surf} play a unique role in identifying the transport and magnetotransport properties of the studied samples.

Acknowledgements Open access funding provided by Uppsala University.

Compliance with ethical standards

Conflicts of interest There are no conflicts to declare.

References

1. Fatemeh Karimi, Abdollah Fallah Shojaei, Khalil Tabatabaeian, Hassan Karimi-Maleh, Shahryar Shakeri. IET Nanobiotechnol. **12**, 336–342 (2018)
2. L. Maftoon-Azad, Z. Yazdanpanah, H. Mohamadi-Baghmolay, A perturbed hard sphere chain equation of state for refrigerants. J. Mol. Liq. **208**, 122–129 (2015)
3. K. Das, B. Satpati, I. Das, The effect of artificial grain boundaries on magneto-transport properties of charge orderedferromagnetic nanocomposites. RSC Adv. **5**, 27338–27346 (2015)
4. P. Dey, T.K. Nath, Effect of grain size modulation on the magneto- and electronic transport properties of $La_{0.7}Ca_{0.3}MnO_3$ nanoparticles: the role of spin-polarized tunneling at the enhanced grain surface. Phys. Rev. B. **73**, 214425 (2006)
5. Y. Zhou, X. Zhu, S. Li, Effect of particle size on magnetic and electric transport properties of $La_{067}Sr_{033}MnO_3$ coatings. Phys. Chem. Chem. Phys. **17**, 31161 (2015)
6. A. Krichene, W. Boujelben, S. Mukherjee, P.S. Solanki, N.A. Shah, Transport and magnetoresistance studies on polycrystalline $La_{0.4}Dy_{0.1}Ca_{0.5}MnO_3$: role of phase separation. J. Acta Mater. **131**, 491–498 (2017)
7. C. Zener, Interaction between the d-shells in the transition metals. II. Ferromagnetic compounds of manganese with perovskite structure. Phys. Rev. **82**, 403 (1951)
8. H.Y. Hwang, S.W. Cheong, N.P. Ong, B. Batlogg, Spin-polarized intergrain tunneling in $La_{2/3}Sr_{1/3}MnO_3$. Phys. Rev. Lett. **77**, 2041 (1996)
9. P. Raychaudhuri, T.K. Nath, A.K. Nigam, R. Pinto, A phenomenological model for magnetoresistance in granular polycrystalline colossal magnetoresistive materials: the role of spin polarised tunnelling at the grain boundaries. J. Appl. Phys. **84**, 2048 (1998)
10. P. Raychaudhuri, K. Sheshadri, P. Taneja, S. Bandyopadhyay, P. Ayyub, A.K. Nigam, R. Pinto, S. Chaudhary, S.B. Roy, Spin-polarized tunneling in the half-metallic ferromagnets $La_{0.72-x}Ho_xSr_{0.3}MnO_3$ (x = 0 and 0.15): experiment and theory. Phys. Rev. B. **59**, 13919 (1999)
11. N. Zhang, W. Ding, W. Zhong, D. Xing, Y. Du, Tunnel-type giant magnetoresistance in the granular perovskite $La_{0.85}Sr_{0.15}MnO_3$. Phys. Rev. B. **56**, 8138 (1997)
12. H.Y. Hwang, S.W. Cheong, P.G. Radeilli, M. Marezio, B. Batlogg, Lattice effects on the magnetoresistance in doped $LaMnO_3$. Phys. Rev. Lett. **75**, 914 (1995)
13. S. Lee, H.Y. Hwang, B.I. Shraiman, W.D. Ratcliff II, S.W. Cheong, Intergrain magnetoresistance via second-order tunneling in perovskite manganites. Phys. Rev. Lett. **82**, 4508 (1999)
14. R. Skini, M. Khlifi, E.K. Hlil, Efficient composite magnetocaloric material with a tunable temperature transition in K-deficient manganites. J. RSC Adv. **6**, 34271 (2016)
15. A.K.M. Akther Hossain et al., Infuence of grain size on magnetoresistance properties of bulk $La_{0.67}Ca_{0.33}MnO_{3-\delta}$. J. Magn. Magn. Mater. **192**, 263–270 (1999)
16. S.P. Isaac, N.D. Mathur, J.E. Evetts, M.G. Blamire, Magnetoresistance of artificial $La_{0.7}Sr_{0.3}MnO_3$ grain boundaries as a function of misorientation angle. Appl. Phys. Lett. **72**, 2038 (1998)
17. R.D. Sanchez, J. Rivas, C. Vazquez-Vazquez, A. Lopez-Quintela, M.T. Causa, M. Tovar, S. Oseroff, Giant magnetoresistance in fine particle of $La_{0.67}Ca_{0.33}MnO_3$ synthesized at low temperatures. Appl. Phys. Lett. **68**, 134 (1996)
18. S. Das, P. Chowdhury, T.K. GunduRao, D. Das, D. Bahadur, Influence of grain size and grain boundaries on the properties of $La_{0.7}Sr_{0.3}Co_xMn_{1-x}O_3$. Solid State Commun. **121**, 691 (2002)
19. A. Gupta, G.Q. Gong, G. Xiao, P.R. Duncombe, P. Lecoeur, P. Trouilloud, Y.Y. Wang, V.P. Dravid, J.Z. Sun, Grain-boundary effects on the magnetoresistance properties of perovskite manganite films. Phys. Rev. B. **54**, R15629 (1996)
20. L. Joshi, S. Keshri, Enhanced CMR properties of $La_{0.67}Ca_{0.33}MnO_3$ sintered at different temperatures. Phase Transit. **83**, 263–275 (2010)
21. E. Rozenberg, M. Auslender, I. Felner, G. Gorodetsky, Low-temperature resistivity minimum in ceramic manganites. J. Appl. Phys. **88**, 2578–2582 (2000)
22. F. Guinea, A. de Andres, J.L. Martinez, C. Prieto, L. Vazquez, M. Garcia-Hernandez, Coulomb blockade versus intergrain resistance in colossal magnetoresistivemanganite granular films. Phys. Rev. B **61**, 9549–9552 (2000)
23. J. Fontcuberta, B. Martinez, X. Obradors, L. Balcells, High-field magnetoresistance at interfaces in manganese perovskites. Phys. Rev. B **58**, 14697 (1998)
24. J.S. Helman, B. Abeles, Tunneling of spin-polarized electrons and magnetoresistance in granular Ni films. Phys. Rev. Lett. **37**, 1429 (1976)
25. M.I. Auslender, E. Rozenberg, A.E. Karlin, B.K. Chaudhuri, G. Gorodetsky, The nature of the low-temperature minimum of resistivity in ceramic manganites. J. Alloys Compd. **326**, 81 (2001)
26. M.I. Auslender, A.E. Kar'kin, E. Rozenberg, G. Gorodetsky, Low-temperature resistivity minima in single-crystalline and ceramic $La_{08}Sr_{02}MnO_3$: mesoscopic transport and intergranular tunneling. J. Appl. Phys. **89**, 6639 (2001)
27. O. Ciftja, M. Luban, M. Auslender, J.H. Luscombe, Equation of state and spin-correlation functions of ultrasmall classical Heisenberg magnets. Phys. Rev. B **60**, 10122 (1999)
28. P. Sheng, B. Abeles, Y. Arie, Hopping conductivity in granular metals. Phys. Rev. Lett. **31**, 44 (1973)
29. R. Mahendiran, R. Mahesh, A.K. Raychaudhuri, C.N.R. Rao, Resistivity, giant magnetoresistance and thermopower in $La_{0.7}Sr_{0.3}MnO_3$ showing a large difference in temperatures corresponding to the ferromagnetic transition and the insulator-metal transition. Solid State Commun. **99**, 149–152 (1996)
30. G. Venkataiah, D.C. Krishna, M. Vithal, S.S. Rao, S.V. Bhat, V. Prasad, S.V. Subramanyam, P.V. Reddy, Effect of sintering temperature on electrical transport properties of $La_{0.67}Ca_{0.33}MnO_3$. Phys. B **357**, 370–379 (2005)
31. A. Urushibara, Y. Moritomo, T. Arima, A. Asamitsu, G. Kido, Y. Tokura, Insulator-metal transition and giant magnetoresistance in $La_{1-x}Sr_xMnO_3$. Phys. Rev. B. **51**, 14103 (1995)
32. V. Sen, N. Panwar, G.L. Bhalla, S.K. Agarwall, Structural, magnetotransport and morphological studies of Sb-doped $La_{2/3}Ba_{1/3}MnO_3$ ceramic perovskites. J. Phys. Chem. Solids **68**, 1685 (2007)
33. G.J. Snyder, R. Hiskers, S. DiCarolis, M.R. Beasley, T.H. Geballe, Intrinsic electrical transport and magnetic properties of $La_{0.67}Ca_{0.33}MnO_3$ and $La_{0.67}Sr_{0.33}MnO_3$ MOCVD thin films and bulk material. Phys. Rev. B. **53**, 14434 (1996)
34. G. Venkataiah, P. Venugopal Reddy, Structural, magnetic and magnetotransport behavior of some Nd-based perovskite manganites. Solid State Commun. **136**, 114 (2005)
35. R. Skini, M. Khlifi, M. Wali, E. Dhahri, E.K. Hlil, Electrical transport and giant magnetoresistance in $La_{0.82-x}{-}_xCa_{0.2}MnO_3$ (x = 0; 0.1 and $x = 0.2$) oxides. J. Magn. Magn. Mater. **324**, 217–223 (2014)
36. M. Wali, R. Skini, M. Khlifi, M. Bekri, E. Dhahri, E.K. Hlil, Double metal-insulator transitions and magnetoresistance properties in $La_{0.8}Na_{0.2-x}{-}_xMnO_3$ oxides. Ceram. Int. **42**, 5699–5706 (2016)

37. A. Dutta, N. Gayathri, R. Ranganathan, Effect of particle size on the magnetic and transport properties of $La_{08.75}Sr_{0.125}MnO_3$. Phys. Rev. B. **68**, 054432 (2003)
38. G. Venkataiah, Y.K. Lakshmi, V. Prasad, P.V. Reddy, Influence of particle size on electrical transport properties of $La_{0.67}Sr_{0.33}MnO_3$ manganite system. J. Nanosci. Nanotechnol. **7**, 2000–2004 (2007)
39. D.L. Mills, Surface effects in magnetic crystals near the ordering temperature. Phys. Rev. B. **3**, 3887 (1971)
40. G. Bergmann, Transition from pauli paramagnetism to band ferromagnetism in very thin Ni films. Phys. Rev. Lett. **41**, 264 (1974)
41. J.M.D. Coey, Noncollinear spin arrangement in ultrafine ferrimagnetic crystallites. Phys. Rev. Lett. **27**, 1140 (1971)
42. J.H. Park et al., Magnetic properties at surface boundary of a half-metallic ferromagnet $La_{0.7}Sr_{0.3}MnO_3$. Phys. Rev. Lett. **81**, 1953 (1998)
43. Y.-A. Soh, G. Aeppli, N.D. Mathur, M.G. Blamire, Mesoscale magnetism at the grain boundaries in colossal magnetoresistive films. Phys. Rev. B. **63**, 020402 (2000)